

Elliptic Flow and Fixed p_T Suppression in a Final State Interaction Model

A. Capella

Laboratoire de Physique Théorique¹

Université de Paris XI, Bâtiment 210, 91405 Orsay Cedex, France

E. G. Ferreira

Departamento de Física de Partículas, Universidad de Santiago de Compostela,
15782 Santiago de Compostela, Spain

Abstract

It has been shown that a final state interaction model, used to describe J/ψ suppression, can also describe the fixed p_T suppression of the π^0 (and charged pions) yield at all values of p_T , with a final state interaction cross-section σ close to one milibarn. We propose an extension of the model to the pion motion in the transverse plane – which introduces a dependence of the suppression on the azimuthal angle θ_R . Using the same value of σ , we obtain values of the elliptic flow v_2 close to the experimental ones, for all values of p_T , including the soft p_T region.

LPT-Orsay-06-12

February 2006

¹Unité Mixte de Recherche UMR n° 8627 - CNRS

1 Introduction

Statistical QCD (i.e. QCD applied to a system in thermal equilibrium) on a lattice predicts the existence of a new phase of matter, quark matter or quark gluon plasma. It is therefore most important to find signals of the thermalization in the heavy ion data. To achieve thermalization is by no means trivial. High densities are only a necessary condition. Strong final state interaction is also needed, as well as an interaction time long enough for the system to equilibrate.

Nuclear collisions are, a priori, not favorable to produce a thermalized system. Indeed, pA collisions can be described with independent string models [1]. There is no indication in the data of final state interaction between particles produced in different strings – despite the fact that the proton collides with several nucleons of the nucleus and densities several times larger than the proton proton one are reached and that several strings are produced in a transverse area of 1 fm^2 .² In a central AA collision this string density is higher and “cross-talk” between different strings is expected. Correspondingly, final state interaction is seen in the data : strangeness enhancement, J/ψ suppression, large p_T suppression, elliptic flow, etc. cannot be described with independent strings. It could happen that string interaction is so strong that the very concept of string becomes meaningless. On the contrary, in view of the nuclear transparency observed in pA , one could expect that final state interaction will take place with a comparatively small cross-section. In this case the bulk of the produced particles is hardly affected by the final state interaction. Only rare events, of the type mentioned above, are strongly modified.

Heavy ion data lend support to this scenario. For instance, one could expect that thermalization strongly affects the p_T distribution of produced particles – especially at low p_T . Experimentally, the variation of $\langle p_T \rangle$ between the most peripheral and the most central collisions is quite small (about 20 % at RHIC) and consistent with the small increase observed in pA . Also the RHIC data on \bar{p}/h^- are flat from peripheral to central collisions – showing no sign of strong $\bar{p}p$ annihilation which would produce a change in the \bar{p}/h^- ratio for (out of equilibrium) peripheral collisions followed by a flatness when thermalization is reached. Turning to rearer

²This is probably due to the small transverse size of the string as characterized by the correlation length of the non-perturbative interaction (about 0.2 fm from lattice data).

events, the centrality dependence of the ratios B/h^- and \overline{B}/h^- at RHIC shows no sign of saturation – increasing monotonically from peripheral to central collisions for Λ , Ξ and Ω – contrary to statistical model predictions [2]. Also the decrease of $\langle p_T^2 \rangle$ of J/ψ at large centralities, predicted in a deconfining phase transition scenario, is not seen in the data [3].

One of the main arguments for (early, transverse) thermalization at RHIC is the description of elliptic flow data with an ideal (no viscosity) hydrodynamical model. However, this view has recently been challenged [4]. Experimentally [5], it turns out that ideal hydrodynamics describes the v_2 data only in a small low- p_T interval and a very small rapidity range. Moreover, it only describes the minimum bias data and fails to reproduce the centrality dependence. In particular, it overestimates the data at small impact parameter, where the densities are higher. A review of hydrodynamic model [6], coalescence model [7] and transport model [8] calculations and its comparison with experimental data, as well as a comprehensive list of references on these models can be found in [5].

Quantitative support to the idea of a weak final state interaction, which affects only rare events can be found in refs. [9] and [10]. In [9] it has been shown that the strangeness enhancement data [11] can be described with a final state interaction cross-section $\sigma = 0.2$ mb. In [10], the J/ψ suppression at CERN-SPS [12] is reproduced with $\sigma = 0.65$ mb. More recently, it has been shown [13] that the large p_T suppression of π^0 's, observed at RHIC can be reproduced with the same final state interaction model [9] [10], using an effective cross-section of the order of 1 mb. In this formalism the ratio $R_{AA}(b, p_T) = dN^{AA}/dy(b, p_T)/n(b)dN^{pp}/dy$ (where $n(b)$ is the average number of binary collisions at fixed impact parameter b) can be reproduced at all values of p_T – including the soft p_T region. Moreover, the large p_T results turn out to be rather insensitive to the value of the p_T shift of the π^0 resulting from its interaction with the hot medium. (In our approach the results for charged pions and π^0 's are identical).

In this paper we propose an extension of the final state interaction model [9, 10, 13] in order to take into account the motion of the pion in the transverse plane. This introduces a dependence of the pion survival probability on its azimuthal angle θ_R , which, in turn, gives rise to a (positive) contribution to the elliptic flow v_2 .

The fact that the mechanism responsible for the large p_T suppression does give a contribution to the elliptic flow at large p_T of the order of the experimental one is known [14] [15]. Here we show that, in the model [9, 10, 13], values of v_2 very close to the experimental ones are obtained in the whole p_T region, including the low p_T one, using the same value of the final state interaction cross-section (of the order of 1 mb) needed to reproduce the experimental values of R_{AA} .

Although this contribution to v_2 results from an asymmetry in the azimuthal angle, it can be qualified as non-flow [15]. Indeed, the mechanism from which it arises (fixed p_T suppression) is maximal at zero impact parameter and, moreover, thermalization is not needed.

2 The final state interaction model

As in refs. [9, 10, 13] the model we are going to use is based on the gain and loss differential equations which govern final state interactions. Following [16] we assume boost invariance and dilution in time τ of the (transverse) densities ρ_i due only to longitudinal expansion ($\rho \sim 1/\tau$). We then have [16]

$$\tau \frac{d\rho_i}{d\tau} = \sum_{k,\ell} \sigma_{k\ell} \rho_k \rho_\ell - \sum_k \sigma_{ik} \rho_i \rho_k . \quad (1)$$

Here $\rho_i \equiv dN^{AA \rightarrow i}(b)/dyd^2s$ are transverse densities and σ_{ij} are the final state interaction cross-sections averaged over the relative velocities of the incoming particles. The first term of (1) describes the gain in type i particle yield resulting from the interaction of k and ℓ . The second one corresponds to the loss of type i particles resulting from its interaction with particle k . Eqs. (1) have to be integrated between initial time τ_0 and freeze-out time τ_f . The solution depends only on the ratio τ_f/τ_0 . Actually particles $i, j, k, \ell \dots$ can be either hadrons or partons. Indeed, at early times the densities are very high and hadrons not yet formed. Thus, at early times eqs. (1) describe final state interactions at a partonic level. Only at later times, we have interactions of full fledged hadrons and, thus, σ represents an effective cross-section averaged over the interaction time. For this reason formation times – which are not introduced here – do not play an important role.

Let us now consider a π^0 produced at fixed p_T interacting with the hot medium

consisting of charged plus neutrals. We assume that in the interaction, with cross-section σ , the π^0 suffers a decrease in its transverse momentum with a p_T -shift δp_T . This produces a loss in the π^0 yield in a given p_T bin. There is also a gain resulting from π^0 's produced at $p_T + \delta p_T$. Due to the steep fall-off of the p_T spectrum the loss is larger than the gain, resulting in a net suppression of the π^0 yield at a given p_T . In this case there is a single final state interaction channel and eqs. (1) can be solved analytically. Integrating both members of eq. (1) over d^2s , we obtain the following expression for the survivable probability of the π^0 in the medium

$$S_{\pi^0}(y, p_T, b) = \exp \left\{ -\sigma \rho(b, y) \left[1 - \frac{N_{\pi^0}(p_T + \delta p_T)}{N_{\pi^0}(p_T)}(b) \right] \ell n(\rho(b, y)/\rho_{pp}(y)) \right\} . \quad (2)$$

Here $N_{\pi^0}(p_T)$ denotes the yield of π^0 's at a given p_T (see section 3). With $\delta p_T \rightarrow \infty$, the quantity inside the square bracket is equal to one and the gain term vanishes. In this case, the survival probability has the same expression as in the case of J/ψ suppression without $c\bar{c}$ recombination. With $\delta p_T = 0$, the loss and gain terms are identical and the survival probability is equal to one.

The density $\rho(b, y)$ in eq. (2) is given by

$$\rho(b, y) = \frac{dN^{AA}}{dy}(b)/G(b) \quad (3)$$

where the inclusive AA distribution refers to the production of charged plus neutrals and $G(b)$ is an effective transverse area (see below).

The argument of the logarithm in eq. (2) is the ratio of the freeze-out τ_f to the initial time τ_0 . The solution of (1) depends only on the ratio τ_f/τ_0 . We use the inverse proportionality between time and density (see above) to write

$$\tau_f/\tau_0 = \rho_0/\rho_f = \rho(b, y)/\rho_{pp}(y) \quad (4)$$

where the freeze-out density ρ_f has been taken to be the pp one, with

$$\rho_{pp}(y) = 3 \frac{dN^{pp \rightarrow h^-}}{dy} \bigg/ \pi R_p^2 . \quad (5)$$

At $\sqrt{s} = 200$ GeV, $\rho_{pp}(y = 0) = 2.24 \text{ fm}^{-2}$.³

³With this prescription the average value of τ_f/τ_0 is of $5 \div 6$. Thus, if $\tau_0 \sim 1$ fm we obtain a freeze out time $\tau_f \sim 5\text{-}6$ fm.

The densities in eqs. (1)-(4) are computed in the dual parton model [1]. They are given by a linear combination of the average number of participants and of binary collisions. The coefficients are obtained from convolutions of momentum distribution and fragmentation functions. Their numerical values for $Au Au$ collisions at $\sqrt{s} = 200$ GeV at each b are given in [17]. Shadowing corrections, described in detail in [17], are included in the calculation. Finally the geometrical factor $G(b)$, resulting from the integration over d^2s of the two members of eqs. (1), is given by

$$G^{-1}(b) = \int d^2s \frac{dN^{AA}}{dy d^2s} n(b, s) \bigg/ \frac{dN^{AA}}{dy}(b) n(b) \quad (6)$$

where $n(b, s) = \sigma_{pp} T_A(s) T_A(b - s) / \sigma_{AA}(b)$. The nuclear profiles T_A are computed from Woods-Saxon densities [18]. We use the non-diffractive inelastic cross-section $\sigma_{pp} = 34$ mb at $\sqrt{s} = 200$ GeV. In writing eq. (6) we have assumed that the large p_T probe scales with the number n of binary collisions⁴.

3 Numerical results for the π^0 suppression

The suppression of the π^0 yield at fixed p_T is usually presented via the ratio

$$R_{AA}(b, p_T) = \frac{dN^{AA}}{dy}(b, p_T) \bigg/ n(b) \frac{dN^{pp}}{dy}(p_T) . \quad (7)$$

In this paper we shall concentrate on the mid-rapidity region $|y^*| < 0.35$. In order to compute this ratio we have to know its value $R_{AA}^0(b, p_T)$ in the absence of final state interaction. Its p_T integrated value (close to 1/3 for the 10 % most central $Au Au$ collisions) is obtained in the dual parton model with shadowing corrections [13]. Its p_T dependence (p_T broadening) is controlled by two mechanisms. The first one is the decrease of shadowing effects when p_T increases. This produces an increase of $R_{AA}^0(b, p_T)$ towards unity. The second mechanism is the Cronin effect proper, which produces a rise of $R_{AA}^0(b, p_T)$ above unity. In ref. [13] we have used a phenomenological parametrization of both effects of the form

$$R_{AA}^0(b, p_T) = R_{AA}^0(b, p_T = 0) \left(\frac{p_T + p_0^{AA}(b)}{p_T + p_0^{pp}} \right)^{-n} \bigg/ \left(\frac{p_0^{AA}(b)}{p_0^{pp}} \right)^{-n} \quad (8)$$

⁴In the dual parton model at very high energies, $dN^{AA}/dy d^2s$, before shadowing corrections are introduced, is also proportional to the number of binary collisions. In this case, $G^{-1}(b) = \int d^2s [T_{AA}(b, s)]^2 / T_{AA}^2(b)$ is a purely geometrical factor. The results obtained with these two definitions of $G(b)$ are quite similar.

where $p_0(b) = (n - 3)/2 < p_T >_b$, $n = 9.99$ and $< p_T >_b$ is the experimental value of $< p_T >$ at each b [19]. Details of the phenomenological parametrization of the p_T distribution leading to eq. (8) can be found in [13]. The initial suppression $R_{AA}^0(b, p_T)$ obtained from (8) reaches values substantially larger than unity and does not decrease towards one at large p_T (see Fig. 1 ; numerical values are given in [13]).

The value of the π^0 suppression, characterized by the ratio (7), can be computed by multiplying $R_{AA}^0(b, p_T)$ by the π^0 survival probability due to final state interaction, given by eq. (2): $R_{AA}(b, p_T) = R_{AA}^0(b, p_T) S_{\pi^0}(p_T, b)$.

In order to compute the survival probability, we have to define the quantity inside the square brackets in eq. (2). Using the same parametrization of the p_T distribution as in eq. (8) we have

$$\frac{N_{\pi^0}(p_T + \delta p_T)}{N_{\pi^0}(p_T)}(b) = \left(\frac{p_0(b) + p_T + \delta p_T}{p_0(b) + p_T} \right)^{-n}. \quad (9)$$

Note that this quantity represents the gain of particles at a given p_T resulting from the particles or partons produced originally at $p_T + \delta p_T$ and that are shifted due to the interaction with the dense medium. As for eq. (8), this parametrization is extracted from the power-law function proposed in Ref. [19].

We have studied different possibilities for the shift δp_T [13]. In a way, this is equivalent to a test on how the mean energy loss (p_T being E at $y = 0$) behaves with the energy. We have also tried different parametrizations for $R_{AA}^0(b, p_T)$, i.e. the ratio in the absence of final state interaction. We have found that our final result depends little on the form of R_{AA}^0 when we take a p_T -shift of the form $\delta p_T = p_T^\alpha / C$. We have also check that our results for $p_T > 5$ GeV/c are almost independent on the form of the shift.

A reasonable description of the data [20] for all values of p_T has been obtained in [13] using

$$\delta p_T = p_T^{3/2} / (20 \text{ GeV}^{1/2}) \quad (10)$$

and the initial suppression R_{AA}^0 given by eq. (8). Note that, at low p_T , δp_T has to decrease in order to match the dual parton model results. For obvious reasons δp_T is expected to vanish at small p_T .

This p_T shift can be used in the whole range of p_T available. However, as mentioned above, one can also use a constant δp_T for $p_T \gtrsim 6 \div 7$ GeV, without any

significant change in the results [13]. Using (10) in the whole p_T region and a value of $\sigma = 1.3$ mb, we obtain the results shown in Figs. 1 and 2. In Fig. 1 we show our results for $R_{AA}(p_T, b)$, eq. (7), in the centrality bin 0-10 %, using $\sigma = 1.3$ mb. They agree quite well with the available data [20] in the whole p_T region, including the soft one. The corresponding values of the initial suppression $R_{AA}^0(p_T, b)$ are also shown. In Fig. 2 we present our results for the dependence of R_{AA} on the number of participants, N_{part} , for $p_T \geq 4$ GeV. The comparison with the data shows that our model reproduces the centrality dependence.

4 Extension of the model to the transverse motion

In its formulation, the final state interaction model introduced in section 2 takes into account the longitudinal expansion – with no consideration for the motion in the transverse plane. Elliptic flow, on the contrary, results from an asymmetry in the azimuthal angle, and, thus, the motion in the transverse plane plays a fundamental role. The extension of the model to take this transverse motion into account is by no means trivial. To the best of our knowledge a totally satisfactory formulation is not available. In the following, we propose a simple extension of the model taking only into account the different path length of the π^0 in the transverse plane for each value of its azimuthal angle θ_R – measured with respect to the reaction plane. At $y^* \sim 0$, the path length R_{θ_R} , measured from the center of the interaction region (overlap of the colliding nuclei) is given by

$$R_{\theta_R}(b) = R_A \frac{\sin(\theta_R - \alpha)}{\sin \theta_R} \quad (11)$$

where $R_A = 1.05 A^{1/3}$ fm is the nuclear radius and $\sin \alpha = b \sin \theta_R / 2R_A$. Note that eq. (11) is only valid in the region $0 \leq \theta_R \leq 90^\circ$, and the integral in θ_R from 0 to 360° is obtained by integrating from 0 to 90° and multiplying the result by four.

Our ansatz consists in the following replacement in eq. (2)

$$\rho(b, y^* \sim 0) \rightarrow \rho(b, y^* \sim 0) R_{\theta_R} / < R_{\theta_R} > \quad (12)$$

where $< R_{\theta_R} > = \int_0^{90^\circ} d\theta_R R_{\theta_R} / \int_0^{90^\circ} d\theta_R$. This is motivated by the fact that, the duration of the interaction, characterized by the argument of the logarithm in eq.

(2), as well as the density of the medium traversed by the π^0 , are expected to be proportional to the π^0 path length associated to its azimuthal angle θ_R , inside the overlap region of the colliding nuclei. Due to the division by $\langle R_{\theta_R} \rangle$ in (12), the results in Section 3 are practically unchanged.

With the replacement (12), the survival probability of the π^0 , $S_{\pi^0}^{\theta_R}(p_T, b)$, depends on the angle θ_R and the elliptic flow can be obtained as

$$v_2(p_T, b) = \frac{\int_0^{90^\circ} d\theta_R \cos 2\theta_R S_{\pi^0}^{\theta_R}(p_T, b)}{\int_0^{90^\circ} d\theta_R S_{\pi^0}^{\theta_R}(p_T, b)}. \quad (13)$$

Clearly, when the π^0 moves along the reaction plane its path length will have its minimal value and the survival probability its maximal one. On the contrary, for $\theta_R = 90^\circ$ the path length will be maximal and the survival probability minimal. Thus, the resulting value of v_2 is positive.

Using the same value $\sigma = 1.3$ mb of the final state interaction cross-section and the same p_T -shift introduced in section 3 in order to describe the experimental values of $R_{AA}(b, p_T)$, we obtain the values of v_2 versus p_T and centrality shown in Figs. 3, 4 and 5. These results are compared with PHENIX and STAR data [21, 22, 23] for charged hadrons. Notice that the results for identified pions are practically the same at least in the low p_T range [5].

It is quite satisfactory that our results are in agreement with experiment for central and medium central collisions, which contain the bulk of the data. The situation for peripheral collisions is further discussed in Section 5. We also describe v_2 in the low and intermediate p_T region. At $p_T > 3$ GeV our results (dashed line) overestimate the data. A natural way to overcome this problem is discussed in the next section.

5 The large p_T region

Using eq. (8), we have obtained an initial suppression $R_{AA}^0(p_T)$ that increases rapidly towards unit with increasing p_T , reaches values substantially larger than unity and does not decrease towards one at large p_T (see Fig. 1). Such a behaviour is expected in the small p_T region where R_{AA}^0 increases rapidly. As mentioned above

part of this increase is due to the decrease of shadowing when p_T increases and part of it to the Cronin effect. At large p_T , on the contrary, this behaviour is not the conventional one. One rather expects that at large p_T , say $p_T > 5$ GeV, where the shadowing corrections are already quite small, the value of R_{AA}^0 is close or equal to unity – consistent with the smallness of the Cronin effect observed in d -Au as well as in the direct photon production data in Au Au.

The value of the π^0 suppression, characterized by the ratio (7) is computed by multiplying $R_{AA}^0(b, p_T)$ by the π^0 survival probability S_{π^0} due to final state interaction, given by eq. (2). In view of that, it is not possible to determine R_{AA}^0 from the large p_T suppression data alone – since one can change the two factors R_{AA}^0 and S_{π^0} , keeping their product unchanged. On the contrary, we have seen that the values of the elliptic flow v_2 depend only on S_{π^0} . Thus, the combined analysis of both sets of data allows a separate determination of the two factors. We are going to show that only values of R_{AA}^0 close to unity at large p_T can describe both sets of data. Accordingly, we proceed as follows: we use eq. (8) only for small p_T and take $R_{AA}^0(b, p_T \geq 5 \text{ GeV}) = 1$. Since the large p_T suppression is given by the product $R_{AA}^0(p_T)S_{\pi^0}(p_T)$, this change of R_{AA}^0 for $p_T \geq 5$ GeV has to go along with a change in $S_{\pi^0}(p_T)$ – which can be achieved by changing the p_T -shift at large p_T . Let us parametrize it in the form $\delta p_T = p_T^\alpha / C$ with the parameters α and C determined in such a way that the size and (practically flat) shape of the large p_T suppression data is preserved. This is achieved with $\alpha = 0.8$ and $C = 9.5 \text{ GeV}^{-0.2}$. Thus, we shall take

$$\delta p_T = p_T^{0.8} / 9.5 \text{ GeV}^{-0.2} \quad \text{for } p_T \geq 5 \text{ GeV} . \quad (14)$$

Let us note that eqs. (10) and (14) lead to the same value of the p_T -shift at $p_T = 2.9$ GeV. Therefore, in order to have a smooth p_T -shift in the whole p_T region, we are going to use eq. (10) for $p_T < 2.9$ GeV and eq. (14) for $p_T \geq 2.9$ GeV. In the first region ($p_T < 2.9$ GeV) we use the form of the initial suppression $R_{AA}^0(p_T)$ given by eq. (8) and, at large p_T , we take $R_{AA}^0(p_T \geq 5 \text{ GeV}) = 1$. In this way our results for R_{AA} are practically the same, as can be seen in Fig. 1, where we show the form of the two different parametrizations for the ratio R_{AA}^0 – ratio before the interaction – and the resulting R_{AA} . Both parametrizations give similar results concerning the ratio for large p_T , for this reason Fig. 2 remains practically unchanged. However, the

values of v_2 at large p_T are substantially reduced. One obtains the full line in Fig. 3. This shows a saturation of v_2 at $p_T \gtrsim 3$ GeV which is consistent with experiment.

More information on the large p_T values of v_2 and their centrality dependence is provided by the preliminary data on the azimuthal angle dependence $S_{\theta_R}(p_T)$ of the π^0 suppression at different centralities [24]. Our results are given in Fig. 6 and compared with experiment. The agreement with the data is reasonable, indicating that the centrality dependence is approximately reproduced. This is in sharp contrast with the disagreement observed at lower values of p_T (Fig. 4), where our centrality dependence is too weak as compared with the data but in much better agreement with the ones in Fig. 5. This important point has to be clarified.

In the above calculation of v_2 we have evaluated the path length of the π^0 (eq. (11)) at its most probable position in the transverse plane, namely the center of the interaction region determined by the overlap of the two colliding nuclei. In a more accurate calculation, we should evaluate this path length at the point in the transverse plane where the π^0 has been produced. However, we have estimated that the error induced by this approximation is less than 10 %. Indeed, we have checked numerically that moving the π^0 production point along the $\theta_R = 0$ direction the value of v_2 decreases, while, moving it in the $\theta_R = 90^\circ$ one, it increases. The average of these two values of v_2 is close to the one obtained using (11) – although somewhat smaller. The difference increases when one moves away from the center and reaches the 10 % level at the mid points on the two axis. Due to the integration over $T_{AA}(b, s)$ present in our calculation, the average position of the produced π^0 is closer to the center of the interaction region than to the mid-points. Thus, the estimated error is less than 10 %.

While the approximation discussed above overestimates slightly the value of v_2 , there is a physical effect which can increase its value in a more substantial way. Namely, if, besides the p_T -shift, the final state interaction produces also a shift $\delta\theta_R$ in the azimuthal angle θ_R of the π^0 , it can be shown that the value of v_2 increases, irrespective of the sign of $\delta\theta_R$. For instance with $|\delta\theta_R| = 15^\circ$, the increase of v_2 at $b = 6$ fm and $p_T = 1.35$ GeV can be as large as 30 %.⁵

⁵The effect depends on the time at which the shift $\delta\theta_R$ takes place. It is maximal when this time is close to freeze-out.

6 Conclusions

We have proposed a final state interaction model which takes into account the different path length of a particle in the transverse plane for each value of its azimuthal angle in the overlap area of the colliding nuclei. The model is an extension of one previously introduced to describe strangeness enhancement, J/ψ suppression and fixed p_T suppression. Using the values of the final state interaction cross-section (about 1 mb) and of the p_T -shift which describe the RHIC data on fixed p_T π^0 suppression, we obtain values of the elliptic flow v_2 close to the measured ones for all values of p_T , including the soft region. As for the centrality dependence, the values of v_2 are well reproduced in the region $b \lesssim 6$ fm which contains the bulk of the data. We argue in Section 5 that the situation for peripheral collisions has to be clarified.

Moreover, combining the analysis of large p_T suppression and elliptic flow data, it is possible to obtain information on the initial suppression, $R_{AA}^0(p_T)$, i.e. the one in the absence of final state interaction – which results from the combined effect of shadowing and the Cronin effect. Values of R_{AA}^0 close to unity at large p_T ($p_T \gtrsim 5$ GeV) are required in order to describe both data sets.

The mass dependence of v_2 is reproduced quite well. The decrease of v_2 with increasing mass is just a consequence of the broadening of the p_T distributions when the mass increases. It will be described in detail in a forthcoming publication [25].

In view of the uncertainties discussed at the end of section 5 we have restricted our calculation to the second order coefficient v_2 and to mid-rapidities. However, our formalism allows to understand qualitatively the strong decrease of v_2 when moving away from mid-rapidities. This decrease follows the decrease of the medium density as expected in our approach. Thus, we expect a dramatic decrease of v_2 when moving away from mid-rapidities.

We do not claim that the mechanism we have introduced gives the only contribution to the elliptic flow. The latter is a very subtle observable to which presumably different mechanisms do contribute. In our opinion, our knowledge of the dynamics of the nuclear interaction is not sufficient to disentangle all these mechanisms and, therefore, to allow to draw clear-cut conclusions regarding the interpretation of the measured values of v_2 .

Together with previous work on strangeness enhancement, J/ψ suppression and fixed p_T suppression, all of which can be described in our framework with final state interaction cross-section smaller than or of the order of 1 mb, this work lends support to the idea that, despite the large densities reached in central $Au Au$ collisions, the final state interaction is rather weak. In terms of string models, it means that there is “cross-talk” between different strings. However, the concept of string remains useful and these models can be used to compute the densities needed as initial conditions in the gain and loss differential equations which govern the final state interaction. Such a weak cross-talk, in the presence of many strings per unit of transverse area, is supported theoretically by the small transverse size of the string – with a radius of the order of 0.1 fm. On the experimental side it is supported by the nuclear transparency of proton-nucleus collisions – where no “cross-talk” is needed to reproduce the data. As a consequence, only rear events are substantially affected but the bulk of the system is not – indicating that the strength and duration time of the final state interaction are not enough to drive the system to thermal equilibration.

Acknowledgments

It is a pleasure to thank N. Armesto, C. Pajares and C. Salgado for interesting discussions and helpful suggestions. We also thank A. Krzywicki and D. Schiff for discussions. E. G. Ferreira thanks the Service de Physique Théorique, CEA, Saclay, for hospitality during the completion of this work.

References

- [1] DPM : A. Capella, U. Sukhatme, C.-I. Tan, J. Tran Thanh Van, Phys. Lett. **B81**, 68 (1979) ; Phys. Rep. **236**, 225 (1994).
QGSMD : A. Kaidalov, K. A. Ter-Martirosyan, Yad. Fiz. **39**, 1545 (1984) ; Yad. Fiz. **41**, 1278 (1985).
- [2] A. Tounsi, K. Redlich, hep-ph/0111159.
J. S. Hamich, K. Redlich, A. Tounsi, Phys. Lett. **B486**, 61 (2000) and J. Phys. G **27**, 413 (2001).
- [3] D. Kharzeev, M. Nardi, H. Satz, Phys. Lett. **B405**, 14 (1997).
N. Armesto, A. Capella, E. G. Ferreira, Phys. Rev. **C59**, 395 (1999).
A. K. Chaudhuri, nucl-th/0212046.
- [4] R. S. Bhalerao, J. P. Blaizot, N. Borghini and J. Y. Ollitrault, Phys. Lett. **B627**, 49 (2005).
- [5] STAR Collaboration, J. Adams et al., nucl-ex/0409033.
- [6] P. F. Kolb, U. Heinz, nucl-th/0305084.
- [7] D. Molnar, S. A. Voloshin, Phys. Rev. Lett. **91**, 092301 (2003).
V. Greco, C. M. Ko, P. Levai, Phys. Rev. Lett. **90**, 202302 (2003).
R. J. Fries, B. Müller, C. Nonaka, S. A. Bass, Phys. Rev. Lett. **90**, 202303 (2003).
R. C. Hwa, C. B. Yang, Phys. Rev. **C70**, 024904 (2004).
D. Molnar, nucl-th/0408044.
S. Pratt, S. Pal, Nucl. Phys. **A749**, 268 (2005); Phys. Rev. **C71** 014905 (2005).
- [8] M. Bleicher, H. Stöcker, Phys. Lett. **B526**, 309 (2002).
Z. W. Lin, C. M. Ko, B. A. Li, B. Zhang, S. Pal, Phys. Rev. **C72**, 064901 (2005).
B. Zhang, M. Gyulassy, C. M. Ko, Phys. Lett. **B455**, 45 (1999).
- [9] A. Capella, C. A. Salgado, D. Sousa, Eur. Phys. J **C30**, 111 (2003).

- [10] A. Capella, D. Sousa, Eur. Phys. J. **C30**, 117 (2003).
A. Capella, E. G. Ferreira, A. Kaidalov, Phys. Rev. Lett. **85**, 2080 (2000).
- [11] STAR Collaboration, C. Adler et al., Phys. Rev. Lett. **87**, 262302 (2001) ; J. Castillo, Nucl. Phys. **A715**, 518c (2003).
- [12] NA50 Collaboration, L. Ramello, Nucl. Phys. **A715**, 243c (2003) ; L. Kluberg in Proc. Quark Matter 2004, Oklahoma, USA.
- [13] A. Capella, E. G. Ferreira, A. Kaidalov, D. Sousa, Eur. Phys. J **C40**, 129 (2005).
- [14] A. Drees, H. Feng, J. Jia, Phys. Rev. **C71**, 034909 (2005).
- [15] A. Dainese, C. Loizides, G. Paié, Eur. Phys. J **C38**, 461 (2005).
- [16] B. Koch, U. Heinz, J. Pitsut, Phys. Lett. **B243**, 149 (1990).
- [17] A. Capella, E. G. Ferreira, Eur. Phys. J **C42**, 419 (2005).
- [18] C. W. Jager, H. De Vries, C. De Vries, Atomic Data and Nuclear Tables **14**, 485 (1974).
- [19] PHENIX Collaboration, S. S. Adler et al., Phys. Rev. **C69**, 034910 (2004).
- [20] PHENIX Collaboration, S. S. Adler et al., Phys. Rev. Lett. **91**, 072301 (2003).
- [21] PHENIX Collaboration, S. S. Adler et al., Phys. Rev. Lett. **94**, 232302 (2005).
- [22] PHENIX Collaboration, S. S. Adler et al., Phys. Rev. Lett. **91**, 182301 (2003).
- [23] STAR Collaboration, J. Adams et al., Phys. Rev. **C72**, 014904 (2005).
- [24] PHENIX Collaboration, D. d’Enterria, Journée Thématique on Jet quenching IPN-Orsay, November 14th, 2005; Eur. Phys. J **C43**, 295 (2005).
- [25] A. Capella and E. G. Ferreira, Proceedings of XL1st Rencontres de Moriond: QCD and High Energy Hadronic Interactions, hep-ph/0604184.

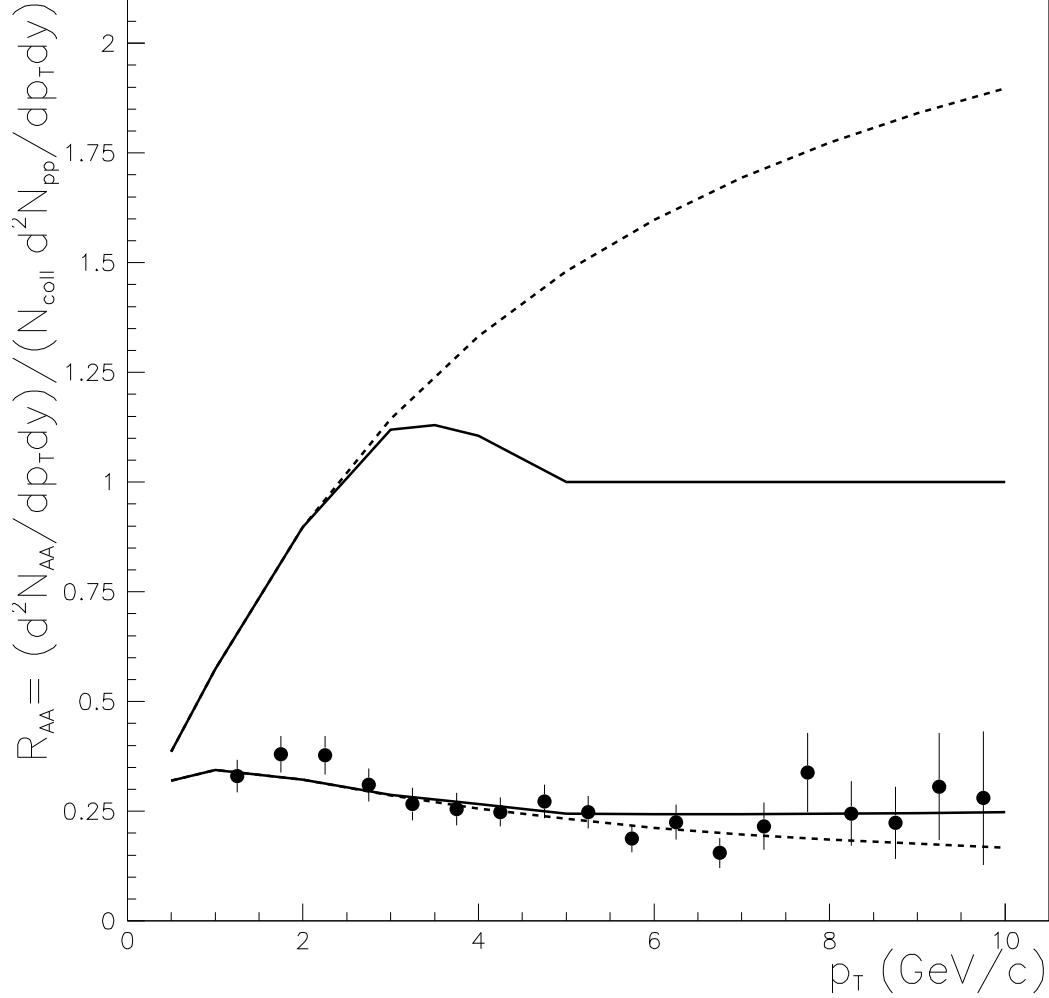


Figure 1: The π^0 suppression factor $R_{AuAu}(p_T, b)$ at $\sqrt{s} = 200$ GeV, eq. (7), versus p_T in the centrality bin 0-10 % and the corresponding π^0 initial suppression factor $R_{AuAu}^0(p_T, b)$ (i.e. in the absence of final state interaction). The dashed lines corresponds to our results obtained using eq. (8) for R_{AuAu}^0 and a p_T -shift given by eq. (10). The continuous lines are obtain with R_{AuAu}^0 described in Section 5 and the p_T -shift given eq. (10) for $p_T < 2.9$ GeV and eq. (14) for $p_T \geq 2.9$ GeV. The data are from [20].

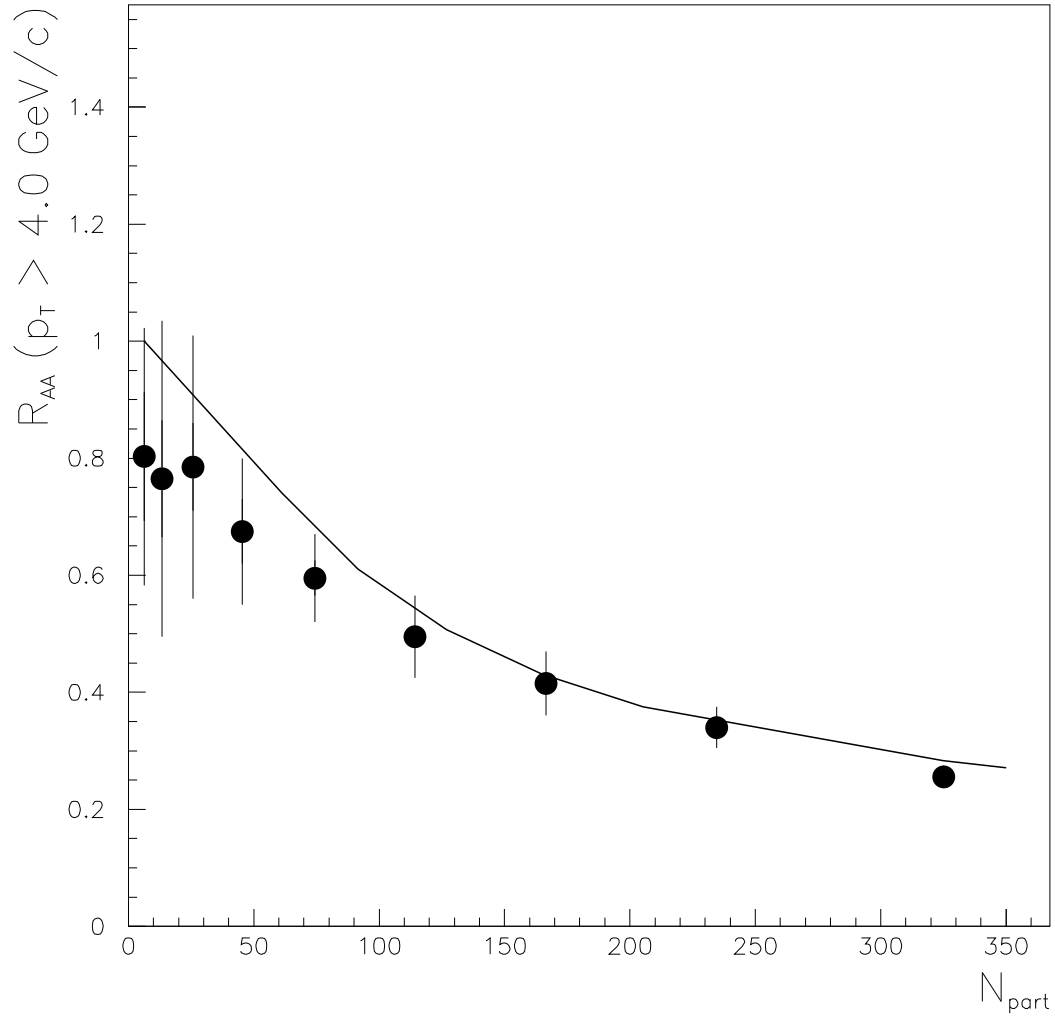


Figure 2: The π^0 suppression factor $R_{AuAu}(p_T, b)$ versus the number of participants, N_{part} , for $p_T \geq 4$ GeV. The data are from [20].

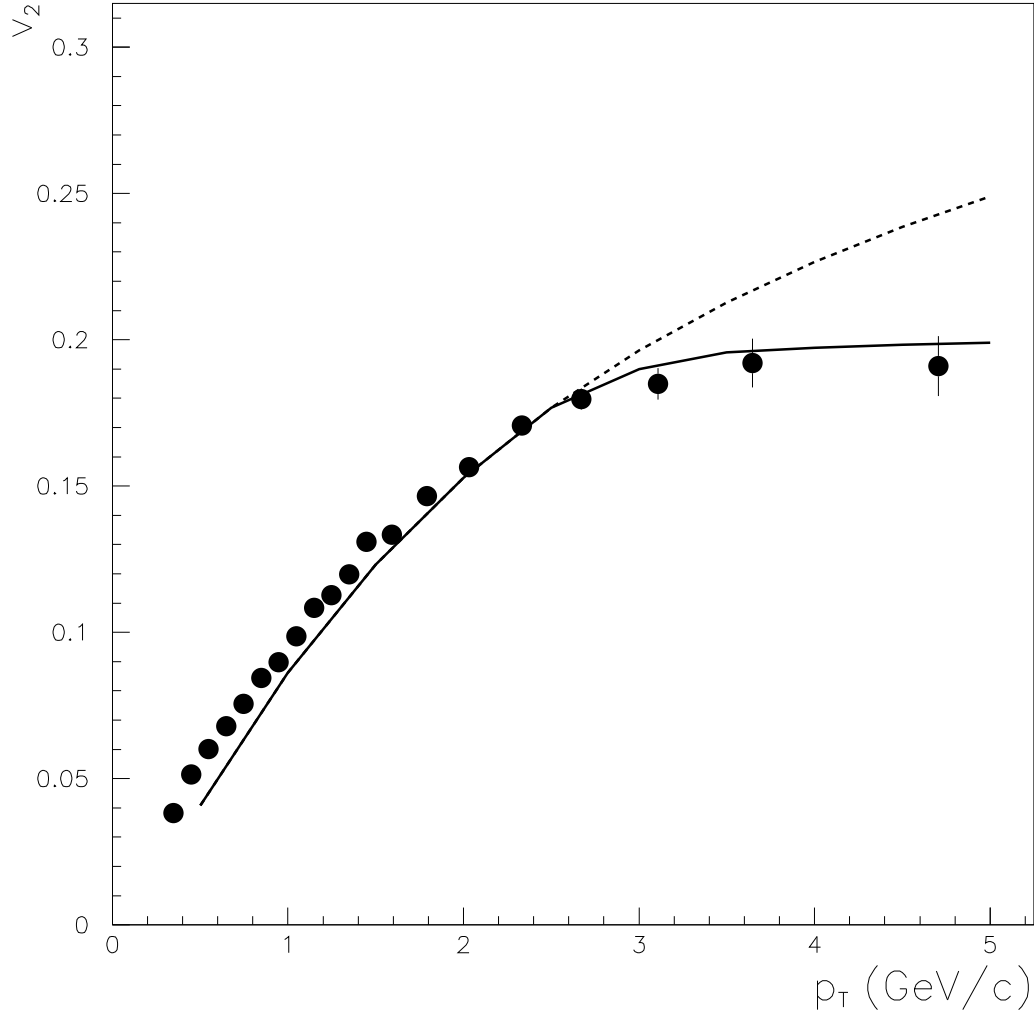


Figure 3: Values of the elliptic flow $v_2(b, p_T)$ versus p_T in the centrality bin 13 %-26 %. The continuous line corresponds to our results obtained using eq. (14), the dashed line corresponds to our results obtained using eq. (10). The data are from [21].

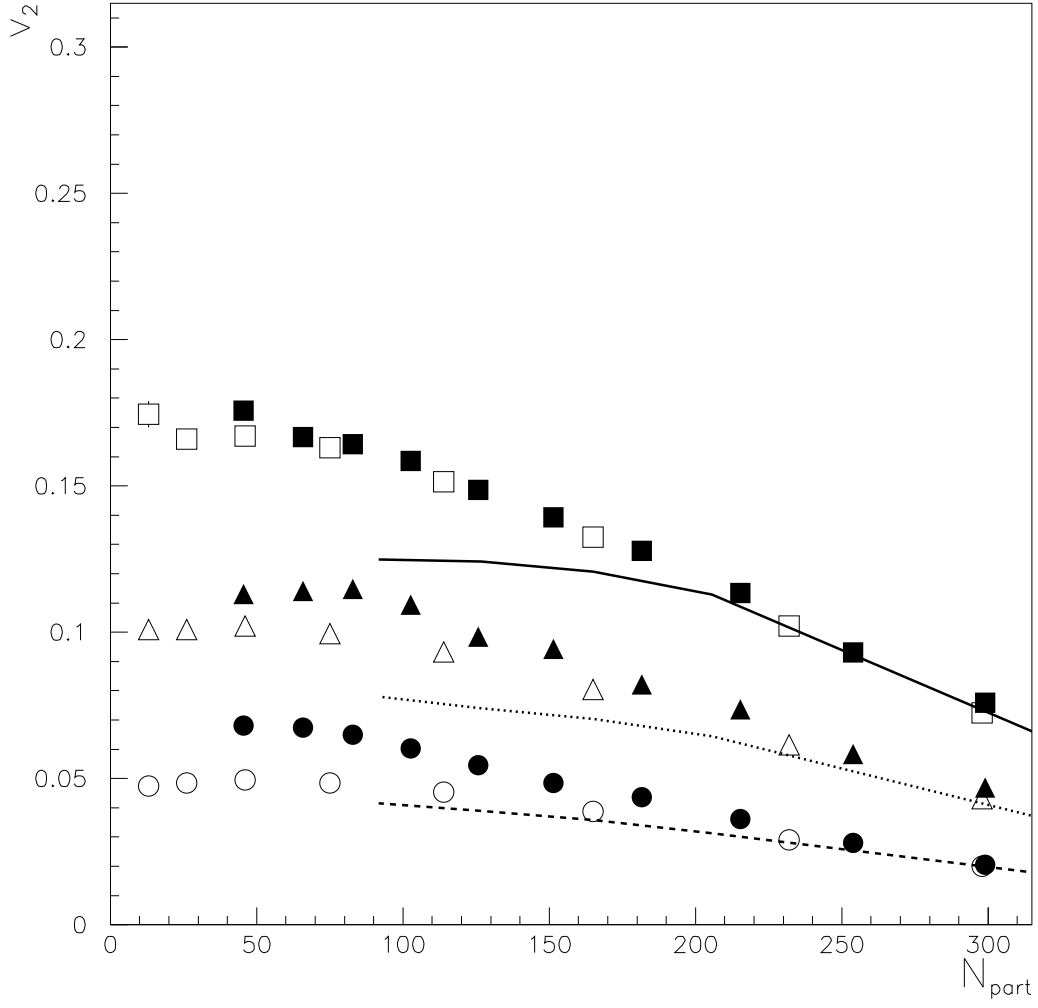


Figure 4: Values of the $v_2(b, p_T)$ versus the number of participants for different values of p_T : $p_T = 0.4$ GeV (lower line), $p_T = 0.75$ GeV (middle) and $p_T = 1.35$ GeV (top). The black data are from PHENIX [21], the open data are from STAR [23].

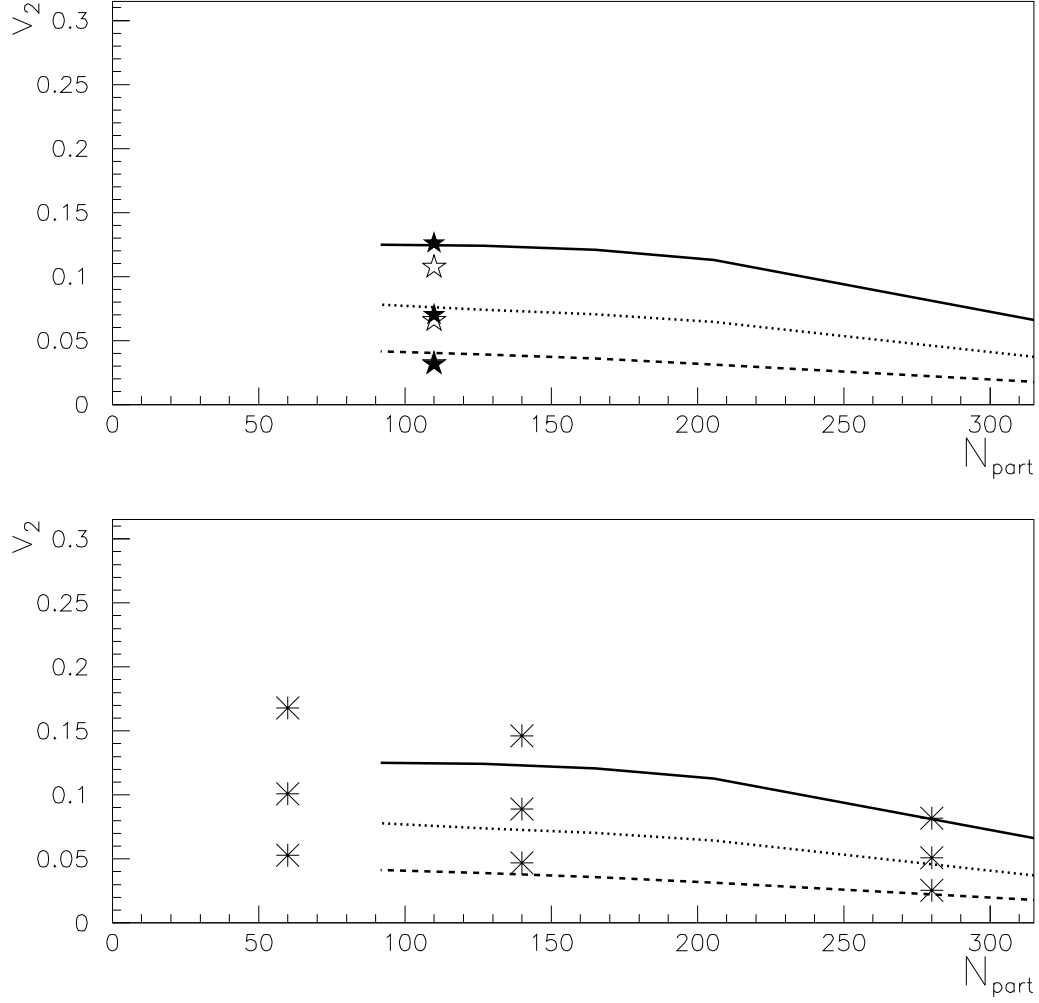


Figure 5: Values of the $v_2(b, p_T)$ versus the number of participants for different values of p_T : $p_T = 0.4$ GeV (lower line), $p_T = 0.75$ GeV (middle) and $p_T = 1.35$ GeV (top) compared to: data in minimum bias collisions from PHENIX [22] (black symbols) and STAR [23] (opened symbols) –above–, data from PHENIX [22] –below–.

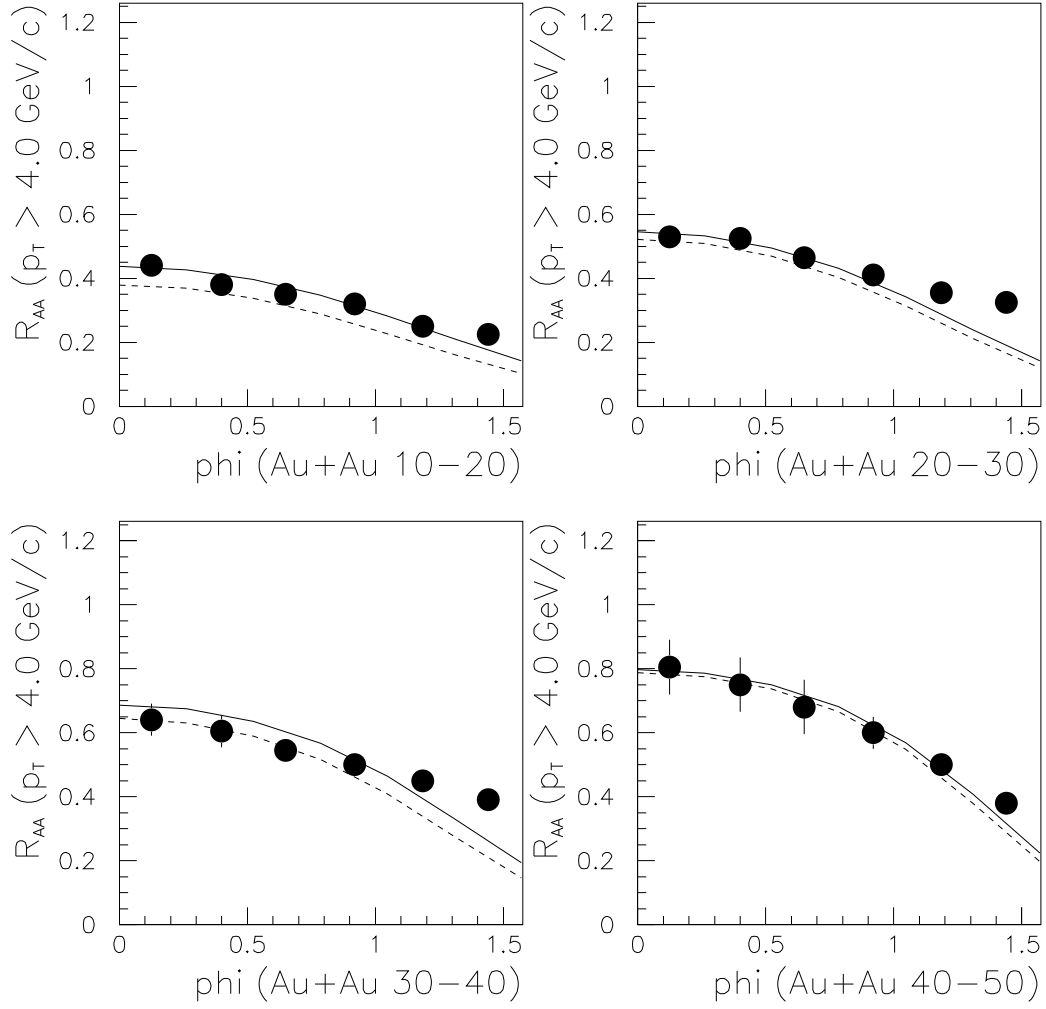


Figure 6: Values of the π^0 suppression $R_{AuAu}(b, \theta_R)$ as a function of the azimuthal angle θ_R (measured from the impact parameter direction) for $p_T \geq 4 \text{ GeV}$ in various centrality bins. The continuous line corresponds to our results obtained using eq. (14), the dashed line corresponds to our results obtained using eq. (10). The preliminary data are from [24].